

Clemson University

TigerPrints

All Theses

Theses

August 2020

The Effect of Varying Environmental Conditions on the Performance of Triboelectric Generators

Andrea Fisher

Clemson University, anfisher@clermson.edu

Follow this and additional works at: https://tigerprints.clemson.edu/all_theses

Recommended Citation

Fisher, Andrea, "The Effect of Varying Environmental Conditions on the Performance of Triboelectric Generators" (2020). *All Theses*. 3401.

https://tigerprints.clemson.edu/all_theses/3401

This Thesis is brought to you for free and open access by the Theses at TigerPrints. It has been accepted for inclusion in All Theses by an authorized administrator of TigerPrints. For more information, please contact kokeefe@clermson.edu.

THE EFFECT OF VARYING ENVIRONMENTAL CONDITIONS ON THE
PERFORMANCE OF TRIBOELECTRIC GENERATORS

A Thesis
Presented to
the Graduate School of
Clemson University

In Partial Fulfillment
of the Requirements for the Degree
Master of Science
Packaging Science

by
Andrea Fisher
August 2020

Accepted by:
Dr. Gregory Batt, Committee Chair
Dr. James Gibert
Dr. Duncan Darby
Dr. Oliver Myers

ABSTRACT

As data creation and collection continues to increase globally, the number of sensors needed to gather data also grows. One thing all types of sensors have in common is their need for power; however, current power sources, like batteries, are limited by their life, size, and weight. To reduce these power limitations, triboelectric energy generators (TENGs) can be used to generate power from the mechanical motion that is present throughout packaged product transport. Triboelectric generation is one such low power mechanism that due to its low cost, has potential in packaging applications. In the distribution environment, packaged products are exposed to a wide range of temperatures and relative humidities. It is important to know how the relative humidities and temperatures seen in packaging distribution environments affect the voltage output of triboelectric energy generators. In order to study relative humidity and temperature effect on TENGs, we mount an optimized triboelectric generator to an electrodynamic shaker located inside an environmental chamber and measure voltage output. This set up allows us to replicate sinusoidal vibration inputs over a wide range of environmental conditions. We found that as relative humidity increases, TENG's root mean square (RMS) voltage output remains essentially the same, and as temperature increases, the TENG's RMS voltage output also remains basically same. We also determined that charge build up is not affected by relative humidity and temperatures found within the packaging distribution environment and that steady state takes longer to establish than a few hundred seconds.

DEDICATION

I dedicate this thesis to my parents, Dave and Stacy Fisher. They have always supported and encouraged me to be the best that I can be. I would not be where I am without them. Guys, we made it.

ACKNOWLEDGMENTS

Thank you to my family and friends who have loved and supported me throughout this journey. It takes a village, and I am lucky to have mine. I love you all.

I would like to thank Dr. Greg Batt, my committee chair, for all the guidance in both undergraduate and graduate school. It means the world to have your support and encouragement throughout my time at Clemson.

To all of the lab, Greg Cocchiola, Davis Ferrell, Aaron Mantia, Ryan McDaniel, Tanner Fogle, Brennan Lytle, Travis Vaughan, and Gary Brown, thank you all for your support and assistance throughout my project. You all are the best.

I am also thankful for my committee members, Dr. James Gibert of Purdue University, Dr. Duncan Darby of Clemson University, and Dr. Oliver Myers of Clemson University. I appreciate all of your counsel throughout my research.

Thanks to Mr. Hongcheng Tao of Purdue University for your help throughout my entire project. I am lucky you have worked with me throughout this journey.

Lastly, I would like to thank Dr. Patrick Gerard for the statistical guidance with data analysis.

I would not have been able to complete this research without you all. Thank you.

TABLE OF CONTENTS

	Page
TITLE PAGE.....	i
ABSTRACT	ii
DEDICATION.....	iii
ACKNOWLEDGMENTS.....	iv
LIST OF TABLES.....	vii
LIST OF FIGURES	viii
CHAPTER	
I. INTRODUCTION.....	1
II. REVIEW OF LITERATURE	6
Triboelectrification	6
Triboelectric Generator Configurations.....	9
Triboelectric Generator Performance Effects.....	14
III. MATERIALS AND METHODS	21
Materials.....	21
Methods.....	27
IV. RESULTS AND DISCUSSION	34
Steady State Charge Comparison	34
Transient Charge Comparison.....	40
V. CONCLUSION	45

Table of Contents (Continued)

	Page
APPENDICES	48
A: Triboelectric Energy Generator Configuration	49
B: Hysteresis in Triboelectric Energy Generators	51
REFERENCES	54

LIST OF TABLES

Table		Page
3.1	The list of test conditions.....	28
4.1	The MANOVA test results	43

LIST OF FIGURES

Figure		Page
2.1	A triboelectric series that is made from combining accepted series	9
2.2	Vertical contact-separation mode is two dissimilar materials moving vertically to create contact and separation.	10
2.3	In-plane sliding mode is two dissimilar materials moving parallel, opposite directions to create a difference in contact area	11
2.4	Single-electron mode is two dissimilar materials, one free moving and one connecting to the ground that creates a flow of electrons to and from the ground.....	13
2.5	Freestanding triboelectric-layer mode is two symmetric electrodes under a dissimilar material that allows free movement energy generation.	14
2.6	Triboelectric energy generator in the form of a tier sheet	18
3.1	The overall setup containing the environmental chamber.	22
3.2	Purdue University 3D printed optimized triboelectric energy generator.....	22
3.3	A triboelectric series that was made from combining accepted series. The materials used in this study are indicated with a box.	23
3.4	An example of an acceptable top TENG platen acceleration plot. Note: The gap in recorded data between recordings for data saving.....	26
3.5	The voltage output of a typical test.	30
3.6	An example of an acceptable top TENG platen acceleration plot.	30
3.7	An example of TENG voltage output analyzed with positive and negative lines of fit. The solid lines are the positive and negative enveloped voltage peaks. The dashed lines are the line of fits of the positive and negative enveloped peaks	32

List of Figures (Continued)

Figure	Page
4.1	TENG steady state RMS voltage during varying relative humidity. 34
4.2	Overview of the studies looking at relative humidity effect on triboelectric energy generators... 37
4.3	TENG steady state RMS voltage during varying temperature. The error bars represent one standard deviation..... 38
4.4	Overview of the studies looking at temperature effect on triboelectric energy generator output performance..... 39
4.5	Relative humidity condition lines of best fit charge build up..... 41
4.6	Temperature condition lines of best fit charge build up..... 42
A-1	A detailed diagram of the triboelectric energy generator created at Purdue University. 50
A-2.1	Initial set up of the two triboelectric generator platens that experienced hysteresis effect.....51
A-2.2	Example of hysteresis effect of the platens made with TPU. 52
A-2.3	Example of no hysteresis effect of the platens made with TPU. 53
A-2.4	Final set up of the two triboelectric generator platens that does not experience hysteresis effect..... 53

CHAPTER ONE

INTRODUCTION

The amount of data created globally is increasing annually. One source predicts that data creation in 2025 will grow to 163 zettabytes (1.63e+13 gigabytes) which is ten times the amount created in 2017 [1]. This global trend includes data collected in the characterization and monitoring of the distribution environment using various types of sensors like GPS trackers, accelerometers, thermocouples, etc. All these sensors have one thing in common; their need for power. Many devices use batteries as their power source, but there are a few limitations with batteries -- battery life, size, and weight. In order to combat these limitations, energy harvesting is being introduced for low power devices [2, 3]. Many different types of energy harvesters exist; however, this study focuses solely on triboelectric energy generators.

Triboelectric energy generators (TENGs) are based on the triboelectric effect. The triboelectric effect is “contact-induced electrification in which a material becomes electrically charged after it is contacted with a different material” [4]. The triboelectric effect can be caused by contact and separation of the two materials or by friction between them, and in many cases, is a combination of both [4, 5]. In this study, the triboelectric energy generator is focused on the contact and separation of two dissimilar materials. Contact electrification, also known as static electrification or contact charging, results in static polarized charges on the two dissimilar materials that contact and separate [5]. TENGs are suggested to need a few hundred cycles of active conditions to generate

consistent/steady-state power through impacts, vibrations, sliding motions, and rotations [6, 7, 8, 9]. The vibrations in a typical packaging distribution cycle are a viable input for triboelectric energy generators. A previous study shows TENGs can power devices like temperature and humidity loggers. There is no mention if TENGs need protection from environmental factors such as various relative humidity and temperature ranges [10].

Throughout a distribution environment, packages are subject to a wide range of environmental conditions. The International Safe Transit Association (ISTA), an association that develops testing standards for laboratory simulation of the various distribution environments of packaged products, recognizes eight different environmental conditions. These conditions have a relative humidity range from 15% to 85% RH and a temperature range from -29°C to 60°C [11]. Leinberger conducted a study to confirm the ISTA temperature range by recording temperatures and relative humidities of shipping containers transported around the world. The data showed that these shipping containers were exposed to temperature ranges of -29°C to 57°C, which is almost identical to the ISTA temperature range. The shipping containers also experienced relative humidity ranges of 32%RH to 96%RH, which overlaps the majority of the ISTA relative humidity range [12]. In October 2018, the Greenville-Spartanburg International Airport (GSP) recorded a relative humidity range of 24% to 100% RH. GSP experiences relative humidities slightly outside of ISTA's range, but these relative humidities are representative of a typical month in Greenville, SC [13]. When triboelectric energy generators are used for a packaging application, it is important to know how these generators will perform when exposed to these varying relative humidity and temperature ranges.

The packaging distribution environment provides an adequate input for the use of triboelectric generators [10]. The frequencies experienced in transportation environment is known to be between 1 – 100 Hz which align with the ideal range of input frequencies of TENGs [21]. Specifically, Wang et al. stated that the ideal input frequency for the TENG mode used in this research, vertical contact separation mode generators, is 5 – 20 Hz [6].

Various researchers have tested triboelectric generators in different relative humidities and temperatures; however, their results are not consistent and some are not complete [10, 14, 15, 16, 17, 18]. The relative humidities used in these studies are within similar ranges as stated by ISTA; however, the studies did not agree upon on the optimal relative humidity level for peak triboelectric energy generator performance. Not all of the studies covered a complete range of distribution environment relative humidities [10, 14, 15, 16]. Nguyen et al. demonstrated the maximum charge created by triboelectric generators decreased more than 20% when the relative humidity increased from 10% to 90% RH [14]. Pence et al. stated that the peaked between 20 – 40% RH [15]. Baytekin et al. found that water is not needed for contact electrification; however, water helps stabilize the surface charge that develops. Baytekin et al. went on to state that lower relative humidity can limit contact electrification more than higher relative humidity after testing 0% RH against ambient conditions (approximately 40% RH) [16]. Barry et. al. tested three different relative humidity levels and found 15% and 35% RH result in similar charge generation of a coin cell battery, while 65 - 70% RH resulted in no charge

generated [10]. In addition to relative humidity, temperature varies throughout a packaged product's distribution environment and requires consideration.

Two research groups concluded that triboelectric energy generators created lower charges in temperatures above 80 – 100°C, however neither were focused on packaging distribution ranges of temperatures [17, 18]. Lu et. al. determined as temperature goes up from -20 to 20°C, charge generated by triboelectric energy generators decreases. Lu et. al. continued to say that as temperatures range between 20°C – 100°C, the charge remains steady, and finally, as temperature increases from 100 – 150°C, the charge continues to decrease [17]. Xu et. al. looked at extremely high temperatures, out of the packaging distribution range, from 353K to 583K. As these extreme temperatures increase, charge decreases [18]. While most studies do not call for further investigation of relative humidities and temperatures, more research is needed to evaluate triboelectric generator performance in the packaging distribution environment.

The problem to be addressed is comparing triboelectric energy generators' steady state performance and charge built up across a range of relative humidities and temperatures encountered in a packaging distribution environment. In order to be a replacement power source for batteries, performance of triboelectric energy generators must be understood over the range of these conditions encountered within distribution. The vibrational inputs encountered in a packaging distribution environment is sufficient to excite a triboelectric energy generator to power a coin cell battery [10]. Relative humidity and temperature's effects on triboelectric energy generators have been studied

[10, 14, 15, 16, 17, 18]; however, no research has been done at the specific relative humidity and temperature ranges seen in a packaging distribution environment.

The goal of this study is to determine the effects of relative humidity and temperature on a triboelectric energy generators' performance during sinusoidal vibration input. This research identifies the optimal relative humidity and temperature for triboelectric energy generators voltage output and compares how voltage builds up over time across different relative humidity and temperatures.

CHAPTER TWO

REVIEW OF LITERATURE

Triboelectrification

The triboelectric effect is defined as “contact-induced electrification in which a material becomes electrically charged after it is contacted with a different material through friction” [4]. This concept of the triboelectric effect has been known since the ancient Greek time of about 2600 years ago [6]. The word triboelectricity comes from the Greek root word *tribos*, meaning to rub, and the word electricity. Triboelectric energy generators (TENG) are based on the triboelectric effect. The triboelectric effect can be caused by contact and separation or of the two materials or by friction between them, and in many cases, is a combination of both [4, 5]. In the past, the triboelectric effect, or triboelectrification, created from friction, has been looked upon negatively. The triboelectric effect has been known to cause ignitions, dust explosions, dielectric breakdown and electronic damage [9]. More specifically, negative examples of triboelectricity include: aircrafts’ radios affected by static charge, cars containing flammable materials need to be discharged to prevent fire, and some electronic devices having the potential to be damaged [4]. However, triboelectrification has also been used in a positive way to generate energy through contact charging. Beginning in the 1800’s, the triboelectric effect was utilized with the Wimshurst machine and the Van de Graff generator to produce high voltage through accumulating static charges. As in future models to come, “triboelectric charges build up an electrostatic field, which drives free electrons to flow through the external load and transfer between the electrodes” [9]. In

early triboelectric energy machines and generators, charges transfer from a rotating belt to a metal brush through corona discharge to create a voltage difference [4]. Once the charge density, electric charge per surface area, in these devices was high enough, they discharged over two opposite electrodes. These early triboelectric generators revealed that if there is no discharge, there is no current, and these devices produce high voltage difference [4].

Recent research has focused on applications for the triboelectric effect. The newer triboelectric nanogenerators use contact electrification and electrostatic induction as a result of mechanical motion to generate energy [9]. These devices can harvest energy through impacts, vibrations, sliding motions and rotations [6, 8, 9]. The generators rely on two dissimilar materials' contact and separation. Upon surface contact of the two dissimilar materials, electrostatic charges are created. This "contact induced triboelectric charge generates a potential drop when the two surfaces" separate. The separation makes electrons move between the electrodes located on the two dissimilar materials [8]. This mechanism is the basis for triboelectric nanogenerators (TENG).

Contact electrification, also known as static electricity or contact charging, results in the static polarized charges on two materials that contact and separate. During the contact and separation, the two materials each develop an opposite charge polarity [5]. Contact electrification can happen between nearly any material, however not all materials will create the same level of charge. Material selection can be a strategic way to generate more charge. This selection refers to a material's position in the triboelectric series. A triboelectric series (TS) lists insulators and organic polymers in order of relative polarity

of the contact charge. The triboelectric series goes from materials that charge most positive at the top to most negative at the bottom [5, 19].

The four most well-known published triboelectric series were published between 1898 – 1987. Each series had a wide variety of synthetic and natural polymers with extremely similar ordering, Fig. 2.1 [5]. The four triboelectric series were combined to form the list below. There are some contradictions with placement of materials across published triboelectric series. For example, Teflon® (PTFE) is a non-polar polymer, however it develops a strong negative charge during contact electrification [5].

More Positive (+)	Glass Mica Polyamind (Nylon 6,6) Rock salt (NaCl) Wool Fur Silica Silk Aluminum Poly (vinyl alcohol) (PVOH) Poly (vinyl acetate) (PVAc) Paper Cotton Steel Wood Amber Poly (methyl methacrylate) (PMMA) Copper Silver Gold Poly (ethylene terephthalate) (Mylar) Epoxy Resin Natural Rubber Polyacrylonitrile (PAN) Poly (vinylidene chloride) (Saran) Polystyrene (PS) Polyethylene (PE) Polypropylene (PP) Poly (vinyl chloride) (PVC) Polytetrafluorethylene (Teflon, PTFE)
(-) More Negative	

Figure 2.1: A triboelectric series that is made from combining accepted series [5].

Triboelectric Generator Configurations

As research has progressed, TENGs have been divided up into four modes, or categories; vertical contact-separation mode, in-plane sliding mode, single-electron mode, and free standing triboelectric-layer mode [6, 8, 9]. Each mode has a different setup of the two dissimilar materials, as well as the movement needed to create energy. These

triboelectric generators all create a voltage output. When a load is placed on the triboelectric generator circuit, power can be calculated. Power is a valuable measurement when identifying devices that can be powered by each specific TENG.

Vertical Contact-Separation Mode

Vertical contact-separation mode uses two different materials with an electrode on each material as shown in Figure 2.2 below. The two materials are set up one on top of the other with connected electrodes: one electrode mounted on the upper of the top material and another electrode mounted on the lower of the bottom material. Upon contact and separation of the two materials, electrons flow back and forth through the electrode to balance the electrostatic field created by the two dissimilar materials [6, 9]. Vertical contact-separation mode TENGs work best with zig-zag, cyclic motion and intermittent impact or shock inputs. These inputs are seen with typing, engines vibrating, walking and biomedical systems like powering a sensor to detect glucose [4, 6, 9].

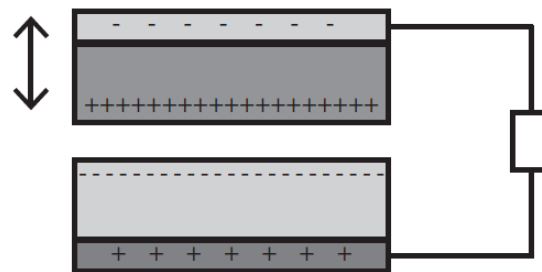


Figure 2.2: Vertical contact-separation mode is two dissimilar materials moving vertically.

In-Plane Sliding Mode

In-plane sliding mode has the same orientation as vertical contact separation mode, but the motion used to create a flow of electrons is horizontal sliding instead of a vertical motion. A diagram is shown in Figure 2.3. The dissimilar materials, with their electrodes attached and connected, are in constant contact. One layer, top or bottom, slide back and forth, to charge the area of the bottom layer that is in contact with the top layer. This sliding motion allows for an unmatched area on the top and bottom layers that creates a mismatch in charges. This mismatch in charges creates a potential difference across the two electrodes, causing electrons to flow to account for the varying charge. Electrons flow back and forth from the electrodes based on the sliding position of the two dissimilar materials. Research suggests that in-plane sliding mode is “more efficient than pure contact” and thus can be considered to have an “enhanced output power for practical applications.” This mode is said to be good for developing more complex designs (compared to other modes) for a higher performance. In-plane sliding mode is the best mode at harvesting energy through planar motions, disc rotations and rotational kinetic energy [4, 9].

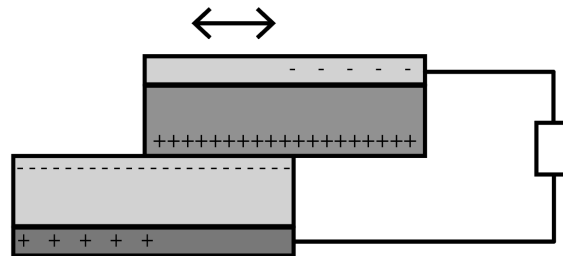


Figure 2.3: In-plane sliding mode is two dissimilar materials moving in parallel, opposite directions to create a difference in contact area.

Single-electron Mode

Single-electron mode addresses an issue that exists with vertical contact-separation mode and in-plane sliding mode: electrodes must be connected. As previously mentioned, electrodes are mounted on the upper of the top material and the bottom of the lower material and. These electrodes are connected, which allows the for the flow of electrons back and forth as shown in Fig. 2.2 and 2.3. Single-electron mode (Fig. 2.4) is made of two dissimilar materials, one free moving and one connected to a ground. The connection to the ground and material-to-material allows for greater freedom of motion compared to vertical contact-separation and in-plane sliding mode. In this mode, the material with a higher surface electron affinity is the free moving material [6, 9]. When the two dissimilar materials are in contact, electrons move from the grounded material to the free moving material because the free moving material has a higher surface electron affinity. Once the free moving material is separated from the grounded material, there is an induced positive charge on the grounded material. This induced positive charge causes electrons to flow from the ground into the grounded material when the free moving material separates from the grounded material. Once the free moving material approaches and comes in contact with the grounded material, electrons flow from the grounded material back into the ground to reestablish electrostatic equilibrium. This cycle continues as the free moving material moves and returns vertically or horizontally. Using single-electron mode, energy can be harvested from flowing air, rotating tires, falling rain, and turning book pages [6, 9].

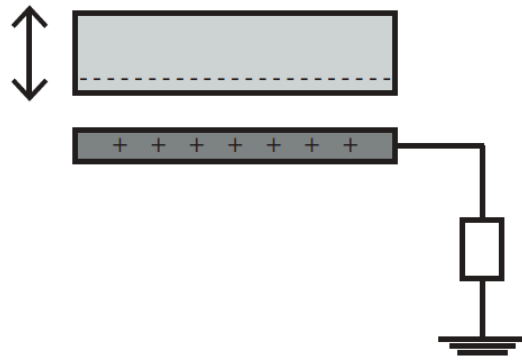


Figure 2.4: Single-electron mode is two dissimilar materials, one free moving and one connecting to the ground that creates a flow of electrons to and from the ground.

Freestanding Triboelectric-Layer Mode

Freestanding triboelectric-layer mode has the advantage of no attached electrodes similar to single-electron mode. In freestanding triboelectric-layer mode, there are two symmetric electrodes under a free moving dissimilar layer as shown in Figure 2.5. Instead of using the ground as a reference electrode, this mode uses pair of symmetric electrodes. There is a small gap between the electrode and dissimilar layer. The approach and departure of the layer above causes an asymmetric charge distribution as electrons flow between electrodes which induces a charge through induction. Freestanding mode can harvest energy from vibration, rotation motions, computer mice movement, air flow, walking and moving cars [6, 9].

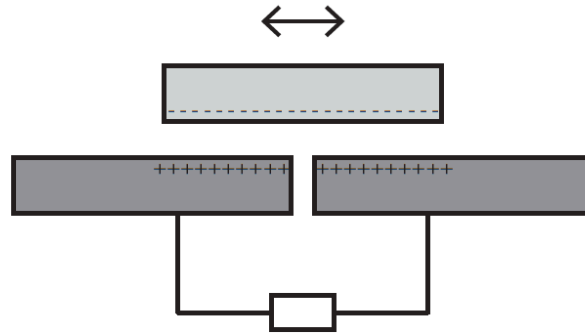


Figure 2.5: Freestanding triboelectric-layer mode is two symmetric electrodes under a dissimilar material that allows free movement energy generation.

Triboelectric Generator Performance Effects

Relative Humidity Effect

When using triboelectric energy generators for a packaging application in a distribution environment, there is a wide range of relative humidities that packages may experience. The International Safe Transit Association (ISTA) is a worldwide organization that set standards in predictive package-performance testing [20]. ISTA develops testing standards to accurately represent distribution environments for packaged products. During the distribution environment, ISTA recognizes packaged products can experience a range of relative humidities. Their testing standards include eight defined conditioning options with relative humidity (RH) ranging from uncontrolled to 15% RH to 85% RH [11]. The Greenville-Spartanburg International Airport reported relative humidity ranging from 24% RH to 100% RH in just one month in October 2018 [13]. These wide ranges of relative humidity all create potential issues for triboelectric electric energy generators. Research groups explore the importance of relative humidity on triboelectric generators, but they do

not agree on the same levels of relative humidity for peak performance of triboelectric generators [10, 5, 6, 14, 15, 16]. One study recommends further research be done to find the ideal operating relative humidity for triboelectric energy generators [10].

A study conducted by Nguyen et al. showed the maximum charge created by triboelectric energy generators was at 0% RH, and the charge generation decreased as RH increases. The TENG developed by Nguyen et al. was made from aluminum and polydimethylsiloxane (PDMS) electrodes (spacer, flexure, and a base). The TENG was placed in a desiccator with controlled RH and pressure. The humidity was controlled by a three-way valve attached to humid air from a water reservoir and dry air from a dry air cylinder to the desiccator. The valve was used to raise or lower the humidity. In this experiment, the humidity was increased or decreased in 10% RH intervals between 10% and 90% RH by feeding in humid air or dry air into the desiccator. When the desired humidity was reached, the valve was shut and closed off humid and dry air sources. The change in humidity was repeated to confirm reproducibility. These published results do not state how many times this study was repeated. The charges from the electrode were measured using an electrometer. This study used an input frequency of 2.5Hz to “acquire data in a reasonable amount of time and to maintain the mechanical stability during the experiment.” Overall, they found charge decreases more than 20% when the RH increases from 10% to 90%RH [14].

Pence et al. found that voltage increased as RH increased from 0 to 20 – 40%, and then voltage decreased once 40% RH was surpassed [15]. They used ion-containing polymeric powders and steel beads to determine the effect of humidity on contact charge

between the two materials. The powder material was a blend of styrene-butyl methacrylate copolymer with minor amounts of the acid form of a sulfonated polystyrene ionomer or the corresponding sodium salt. A mixture of the powder and asymmetrical steel beads was rolled to induce charge. The mixture was rolled in a Faraday cage. The cage was used to ensure no outside factors affect the test. The powder and bead mixture were rolled in the Faraday cage for 30 minutes at 276 rpm in a humidity-controlled environment. After the rotations, the powder was separated from the beads with a dry air stream and the charge of the beads were measured with an electrometer. The humidity was increased/decreased in 10% RH intervals, and the chamber was allowed to stabilize for 30 minutes in between RH changes. Overall, they found at 0% RH, the contact charge on the powder blend was the charge of the copolymer. Above 0% RH, contact charge increased with a humidity increase from 0% to 20 – 40% RH and decreased after 40% RH [15].

Although Diaz et al. found that water is not needed for contact electrification, other studies state a higher charge is often attained in a vacuum and charge significantly decreases in high humidity environments [5]. Baytekin et al. agreed that water is not needed for contact electrification, however water helps stabilize the surface charges that develop. In this study, to have the best contact electrification, they used polytetrafluoroethylene (PTFE), polycarbonate (PC), and polydimethylsiloxane (PDMS) in contact with PDMS. PDMS samples were prepared by casting prepolymer/crosslink mixture on silicon wafer (Si Wafer) and curing the samples in a vacuum overnight at 65°C. The setup utilized two pieces of material and a Faraday cup submerged in dry paraffin oil. The Faraday cup was connected to an electrometer to measure charge. The entire

submersion was placed in a glove-box, in an inert atmosphere created by Argon, and held at ambient temperature (20-25°C) during experimentation. The study showed there was charge generated in the atmosphere with no water, but with atmospheric water, there was greater charge. This study also determined that even though no water was needed for contact electrification, water helped stabilize the charge. The results demonstrated that lower relative humidities limit contact electrification more than higher relative humidities [16].

Barry, et. al. briefly addressed relative humidity in their work with TENGs. While the purpose of this work was to prove feasibility of applying triboelectric generators to a packaging application, they also did five tests in which they attempted to charge coin cell batteries at varying relative humidities [10]. They used a triboelectric harvester that was composed of a generator, Fig. 2.6, and a 3-coin cell battery station. The generator was made of six layers of materials: B-flute corrugate, aluminum coated PE, Teflon (PTFE), circle cushions, aluminum-coated PE and B-flute corrugate. They used 15%, 35%, 35%, 35%, and 65-70% RH. Testing continued in a packaging distribution environment, and the energy harvester was placed in between top levels in a pallet, because it is known that the top area of the pallet maximizes mechanical energy input into the generator [21]. In order to mimic a distribution input, the pallet containing the energy harvesting slip sheet was placed on a servo-hydraulic vibration system. After placement, Barry et al. ran the ISTA Steel Spring Random Vibration Spectrum to replicate a truck trailer movement during transport. Barry et al. repeated the test under different relative humidities. Tests performed at 65-70% RH resulted in no charge increase of the coin cell battery from the beginning to

the end of the test. The results also showed tests performed at 15% RH had the largest increase in charge. Charge generation results from two of the three tests run at 35% RH were extremely close to the amount of charge generation of the single 15% RH test. The change in charge of two of the 35% RH tests differed from the 15% RH test by only 0.01V and 0.03V. Barry et al. suggested that more work needs to be done to further examine the effect of relative humidity on the performance of triboelectric energy generators [10].

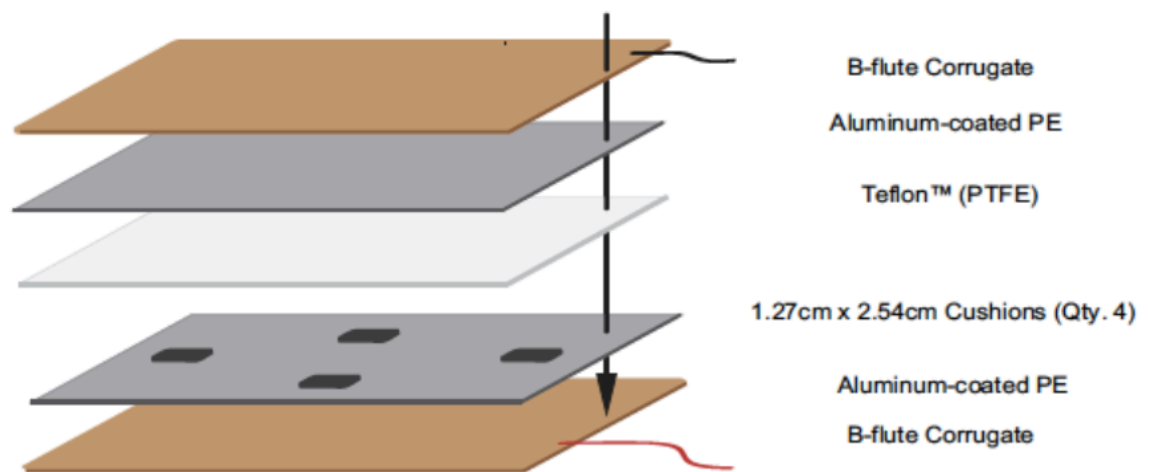


Figure 2.6: Triboelectric energy generator in the form of a tier sheet [10].

These studies present conflicting views on effect of relative humidity and the optimal relative humidity for generating charge in triboelectric energy generators. These conflicting sources suggest a need for more research that focuses on relative humidity effects on TENG performance.

Temperature

When using triboelectric energy generators for a packaging application in a distribution environment, there is a wide range of temperatures that packages have potential to experience throughout the distribution cycle. The ISTA recognizes that packaged products

experience a range of temperatures. The ISTA standards have conditioning temperatures ranging from -29°C to 60°C [11]. While those are part of the eight profiles for testing conditioning, there have been more extreme temperatures documented, such as ocean shipping containers ranging from -29°C to 57°C [12]. There is a wide range of temperatures over which triboelectric energy generators would have to operate at if used throughout the distribution environment. However, there are researchers that disagree on the optimal temperature of a triboelectric energy generator, and other sources encourage further research in order to determine the optimal operating temperature [9, 17, 18, 22].

Lu et al. found that electrical output was highest in colder temperatures and lowest in hot temperatures. In their work, they used a TENG made of aluminum foil, polyethylene terephthalate insulation tapes and PTFE sheets. The PTFE sheet and aluminum foil were attached to two supporting plates with PET insulation tape. This study used single-electron mode TENG to generate charge. The TENG was conditioned and tested inside of a temperature chamber with a RH of $10 \pm 2\%$. In order to re-establish equilibrium, the TENG was conditioned for ten minutes after temperatures are adjusted. The voltage output generated was highest in the extreme cold temperatures. The voltage output dropped from temperatures -20°C to 20°C . The voltage remained steady between 20°C to 100°C and rapidly decreased after 100°C . The decrease in electrical output was explained by change in material permittivity and temperature-induced surface flaws like defluorination and surface oxidation [17].

Xu et al. stated that charge decays at high temperatures. This study did not use a metal-polymer or polymer-polymer TENG because polymer could not withstand the high

temperatures. They used two TENGs made of Ti-SiO₂ and Ti-Al₂O₃ that were able to withstand temperatures of 673 K. Before operating the TENGs, initial charges were induced on SiO₂ and Ti-Al₂O₃ by rubbing polyurethane (PU) and PU-Al₂O₃ respectively. These TENGs were then placed in separate heating cabinets and heated with an accuracy of +/- 5K with a relative humidity less than 30%. The TENGs were held at the determined temperature. The higher the temperature of the cabinet, the faster the TENG lost its residual charge. After the undisclosed waiting period, an input frequency of 2.7 Hz was applied to determine long term charge deterioration at various temperatures. As the temperature increased, the charge deterioration increased as well [18].

CHAPTER THREE

MATERIALS AND METHODS

Materials

Completion of the study objectives required the precise control of temperature and relative humidity during vibration testing of a contact-mode triboelectric generator (TENG). An environmental chamber (PGC, Kings Mountain, NC) was developed with a custom interface to enable sealing around the 19 inch diameter head expander vibration fixture of an electro-dynamic (ED) shaker (Data Physics, San Jose, CA). A fixture designed to contain the TENG was 3D printed and mounted to the ED shaker. A data acquisition system was developed to record TENG voltage output, measure the acceleration of the TENG top mass, and validate ED shaker input. The setup is shown in Fig. 3.1 and 3.2.

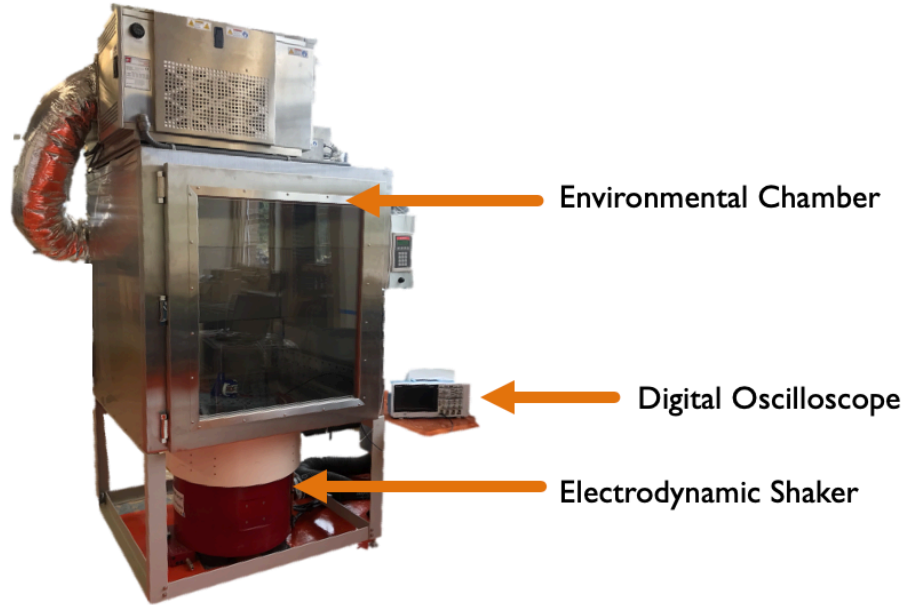


Figure 3.1: The overall setup containing the environmental chamber, electrodynamic shaker, triboelectric energy nanogenerator, and digital oscilloscope.

Triboelectric Energy Generator

The triboelectric energy generator was a custom designed, vertical-contact mode, TENG created at the Advanced Dynamics and MechanicS (ADAMS) lab at Purdue University (West Lafayette, IN), Appendix A and B. This generator design ensured proper mounting to the electrodynamic shaker and consistent alignment of the two dissimilar material surfaces, Fig. 3.2. The fixture was 3D printed with polylactic acid (PLA). The top platen of the TENG was free to slide along a linear rail guide and supported a 200-gram weight and a piezoelectric accelerometer (PCB, Depew, NY).

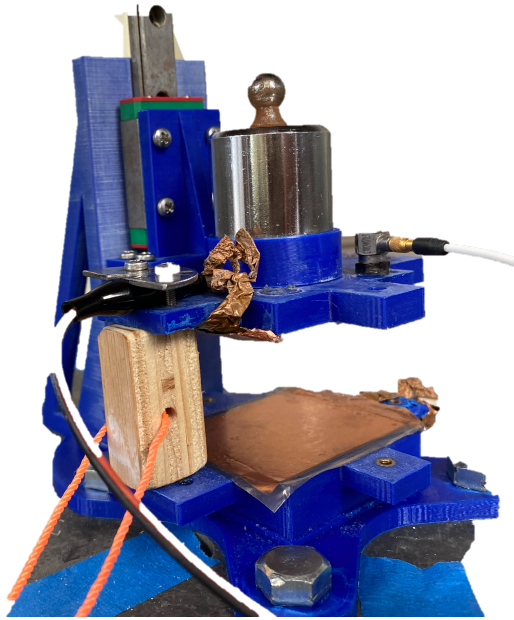


Figure 3.2: Purdue University 3D printed optimized triboelectric energy generator with accelerometer and weight mounted on top platen.

The 200-gram weight ensured forcible contact between the top and bottom platen during excitation. The generator's platens were 50.8 mm square flat surfaces. An accelerometer measured the acceleration of the generator throughout testing to verify consistent contact. The two materials mounted on the two platens of the generator were selected based on their location on the triboelectric series, Fig. 3.3.

More Positive (+)	Glass Mica <div style="border: 2px solid red; padding: 2px;">Polyamind (Nylon 6,6)</div> Rock salt (NaCl) Wool Fur Silica Silk Aluminum Poly (vinyl alcohol) (PVOH) Poly (vinyl acetate) (PVAc) Paper Cotton Steel Wood Amber Poly (methyl methacrylate) (PMMA) Copper Silver Gold Poly (ethylene terephthalate) (Mylar) Epoxy Resin Natural Rubber Polyacrylonitrile (PAN) Poly (vinylidene chloride) (Saran) Polystyrene (PS) Polyethylene (PE) Polypropylene (PP) Poly (vinyl chloride) (PVC) <div style="border: 2px solid red; padding: 2px;">Polytetrafluorethylene (Teflon, PTFE)</div>
(-) More Negative	

Figure 3.3: A triboelectric series that was made from combining accepted series [5]. The materials used in this study are indicated with a box.

Materials selected for this study were polytetrafluoroethylene (PTFE), commonly called Teflon, and Nylon 6,6. Both materials were adhered to separate 50.8 mm wide copper tape (Kraftex, Cotswolds, England), which served as the electrode, Figure 3.4.

The copper tape was 0.065 mm thick, including the conductive adhesive backing. The 3M 5480 Teflon tape (Uline, Pleasant Prairie, WI) was 0.0934 mm thick and taped to one piece of copper tape using its silicone adhesive. Silicone is next to PTFE on the triboelectric series list which made it a good adhesive to use. The Nylon 6,6 film (McMaster-Carr, Elmhurst, IL) was 0.0254 mm thick and adhered with spray adhesive to a different piece of copper tape. In order to create an extension of the copper electrode, a 6.35 mm wide copper tape, 8.85 mm thick, was folded and adhered to the bottom side of each 50.8 mm copper tape to create copper leads. The electrode leads allowed the alligator clips from the digital oscilloscope to attach to the copper electrode without disrupting the surface contact areas. On top of the lower platen, the copper tape was adhered using the tape's conductive adhesive. On top of the lower platen with the copper tape, the Teflon tape was adhered to the top of copper using the Teflon tape's silicone adhesive. On the bottom of the upper platen, the copper tape was adhered using the tape's conductive adhesive. On top of the upper platen with copper tape, the Nylon 6,6 film was adhered with 3M spray adhesive. The 3M spray adhesive was strong enough to ensure the materials remained together throughout the testing. See Fig. 3.4 for the platen set up. Once the material samples were securely adhered to the two platens of the generator, the generator was mounted to the center of the electrodynamic shaker head expander.

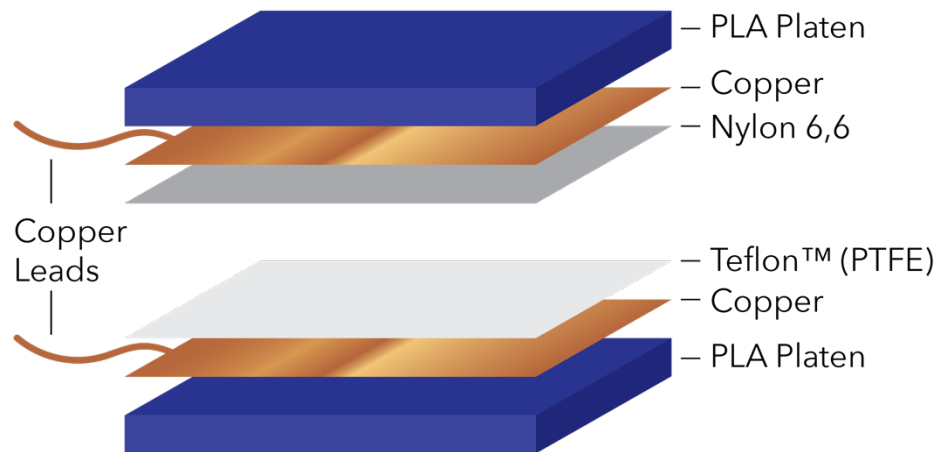


Figure 3.4: Triboelectric generator material layers

Controlled Environment Vibration

The electrodynamic (ED) shaker with an added head expander (DataPhysics, San Jose, CA) was used to generate the sinusoidal vibration input to the TENG which created the contact/separation necessary for electrification. A piezoelectric accelerometer was mounted to the head expander to verify that the input remained consistent throughout testing. An environmental chamber was built up around the circular head expander of the ED shaker to precisely control the surrounding environmental conditions.

The environmental chamber, model: 9325-81R0-BCA0000, (Parameter Generation and Control, Black Mountain, NC) with internal dimensions 1.12 x 0.89 x 1.22 meters was custom built to interface with the ED shaker. The chamber had a circular cut out and a rubber seal on the bottom to enable ED shaker movement while maintaining an air seal. This chamber had an additional dryer installed to expand the range of relative humidities obtainable. The environmental chamber system was able to control conditions down to a dew point of -5°C and was capable of temperatures ranging from 10°C – 30°C and relative humidities ranging from 10% - 85% RH.

Data Acquisition System

The TBS 2074 digital oscilloscope (Tektronix, Beaverton, OR) was connected to the triboelectric generator with alligator clips, and the sampling rate setting was set at 3120 Hz. The minimum sampling rate was calculated using the contact duration of the TENG platens, 5 ms. This duration corresponds to a frequency of 200 Hz. Following the dynamic recording recommendations of SAE J211, the minimum sampling frequency was determined to be 2000 Hz, or ten times the contact frequency. A 3120 Hz sampling rate setting was selected as the closest available sampling rate on the data acquisition system. The maximum number of data points that were able to be exported in a single recording were 2 million. Given the sampling rate and maximum storage, the maximum run time of each exported file was approximately 10.66 minutes. A Tektronix (Beaverton, OR) 10M Ω probe was used to connect the TENG to the oscilloscope. The piezoelectric accelerometer model LW241703 (PCB, Depew, NY) was run through the PCB model 482A22 signal conditioner (Depew, NY) to the oscilloscope.

Methods

Test Procedure

The temperatures and relative humidities tested were based on the conditions that may be present in a packaging distribution environment that also fell within the capability range of the environmental chamber. During the varying relative humidity tests, the temperature was held at 23°C. During the varying temperature tests, the relative humidity was held at 35%RH. Each test condition was repeated three times. The benchmark conditions of 23°C at 35%RH were repeated throughout the test sequence for

a total of 15 times to observe variability and study repeatability. The complete list of test conditions, in order, is listed in Table 3.1.

Table 3.1: The list of test conditions.

Test	RH (%)	Temperature (°C)	Test	RH (%)	Temperature (°C)
1	35	23	19	85	23
2	35	23	20	85	23
3	35	23	21	85	23
4	15	23	22	35	23
5	15	23	23	35	23
6	15	23	24	35	23
7	35	23	25	35	10
8	35	23	26	35	10
9	35	23	27	35	10
10	55	23	28	35	17
11	55	23	29	35	17
12	55	23	30	35	17
13	75	23	31	35	23
14	75	23	32	35	23
15	75	23	33	35	23
16	35	23	34	35	30
17	35	23	35	35	30
18	35	23	36	35	30

Each test was started by cleaning the Nylon and PTFE sides of the triboelectric generator platens with isopropyl alcohol (IPA). IPA has been shown to clean the surfaces of charge [23, 24]. The cleaning method consisted of two sprays of IPA to each platen. The platens were held to allow the excess IPA to drip off the Nylon and PTFE. The remaining IPA was blotted off until the Nylon and PTFE covered platens were dry, and then the generator was mounted to the ED shaker inside the environmental chamber. During the mounting process, separation of the two platens was maintained with a 40 mm block to assure contact electrification did not occur prior to testing. The spacer block only came into contact with the PLA flanges, not the Nylon or PTFE adhered to the

platen. Alligator clips from the digital oscilloscope were attached to the TENG copper wire leads and into the digital oscilloscope with no external resistance load, making an open circuit.

Conditioning the generator prior to testing was a critical step in collecting accurate data. The predetermined relative humidity and temperature conditions were met within $\pm 1\%RH$ and $\pm 1^\circ C$ for three minutes to establish equilibrium. After equilibrium was met, the generator was conditioned for at least ten minutes by allowing the generator to remain idle at set conditions as was done by Lu et al. [17]. When conditioning was completed, the platen spacer block was pulled, using the block's string that was outside of the environmental chamber, the platens came into contact, and the vibration testing was started. Immediately after the platens touched, the test was initiated with the start of the ED shaker. The ED shaker provided an input of $1.4 \pm 0.05g$ at 5 Hz to maximize contact, separation and voltage output of the TENG. Once the ED shaker reached input settings (approximately 12 seconds) the digital oscilloscope began recording. The digital oscilloscope recorded the triboelectric generator voltage output and the triboelectric generator's top platen acceleration for 10.66 minutes. Once the data were saved, a second 10.66-minute recording was obtained. The completion of the second recording concluded the test. A single test, including the time in between recordings, was approximately 22 minutes, Fig. 3.5.

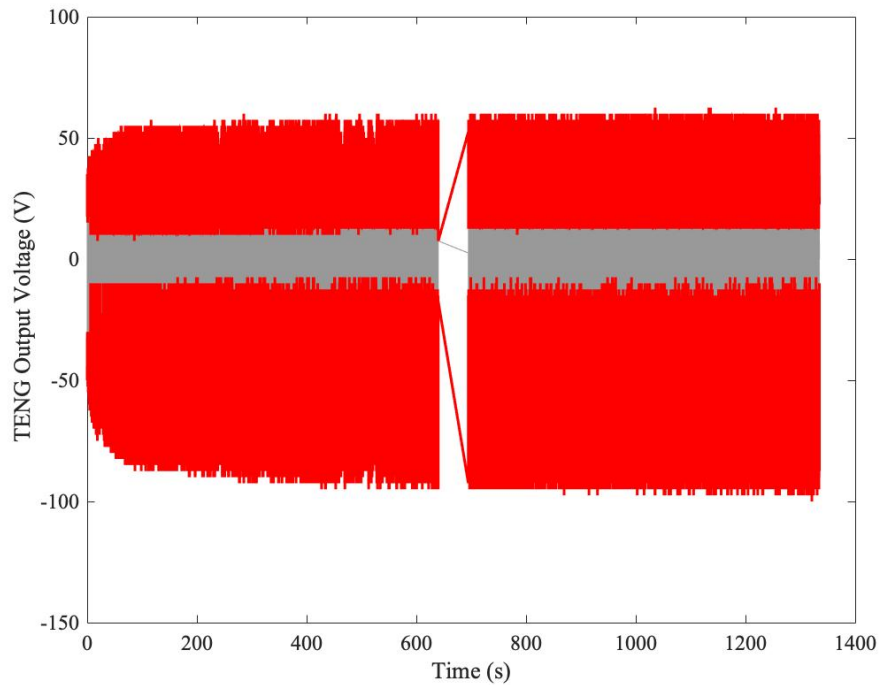


Figure 3.5: The voltage output of a typical test.

Data Analysis

Once the data were recorded, the files were analyzed using MATLAB[®] (MathWorks, Natick, MA). The acceleration signal was analyzed for consistency to ensure the TENG's top platen moved consistently throughout the entire test. An example of a consistent acceleration response is plotted in Fig. 3.6. If platen acceleration variation was visually observed, the test was repeated. Unacceptable platen acceleration would not have consistent acceleration (peaks, low areas, etc.).

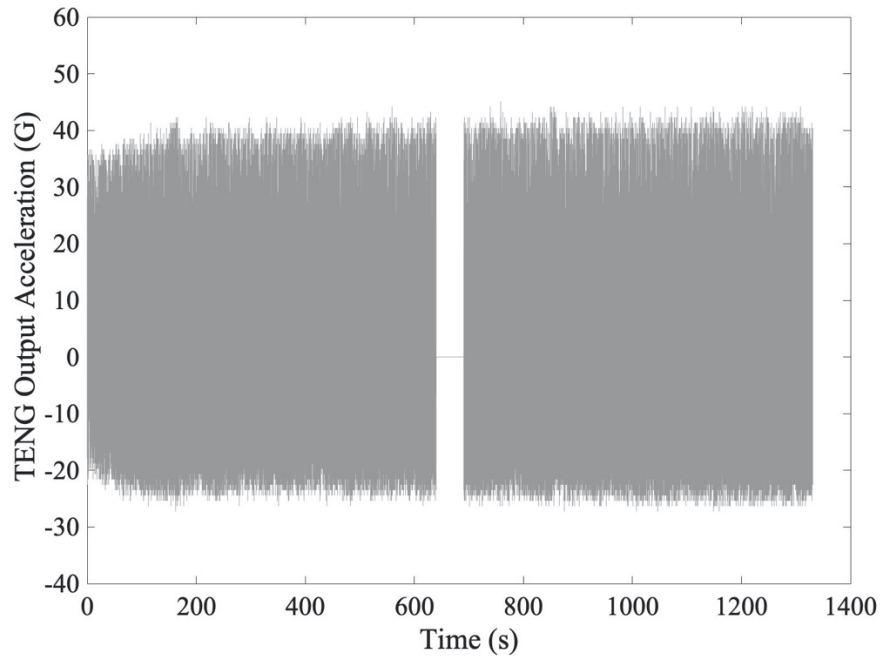


Figure 3.6: An example of an acceptable top TENG platen acceleration plot.

Note: The gap between recordings for data saving/ file writing.

The TENG output was quantified for comparison at various atmospheric conditions by calculating the root mean square (RMS) of the voltage for second 10.66-minute recording. The second recording represented the steady-state voltage output.

The increase in voltage output with time was evaluated by analyzing the first 10.66-minute recording, referred to as the transient voltage output. A multi-step approach was taken to quantify the trend of the TENG voltage build. The FINDPEAKS command in MATLAB[®] was used to determine the positive and negative peaks and then the Hilbert Transform was used to determine the upper and lower envelope of the peaks. Further reduction of the data set was achieved by taking the moving average. The

moving average was weighted heavier in the beginning of the curve when the slope of the exponential curve is greater than at the end of the 10.66-minute segment. These three analytic steps resulted in a positive and negative envelope data set for which exponential curves were fit, Figure 3.7. A two-term exponential curve of the form

$$y = Ae^{Bx} + Ce^{Dx} \quad (3.1)$$

was fit to the resulting data set. The coefficients A, B, C, and D, of the upper and lower peaks across the 36 runs, were compared using a multivariate analysis of variance (MANOVA) statistical test. A MANOVA test was selected as a statistical test because of its ability to test the difference of all four of the variables in Eq. (3.1). MANOVA tests were run using JMP Pro14® to compare positive relative humidity lines of fit, negative relative humidity lines of fit, positive temperature lines of fit, and negative temperature lines of fit.

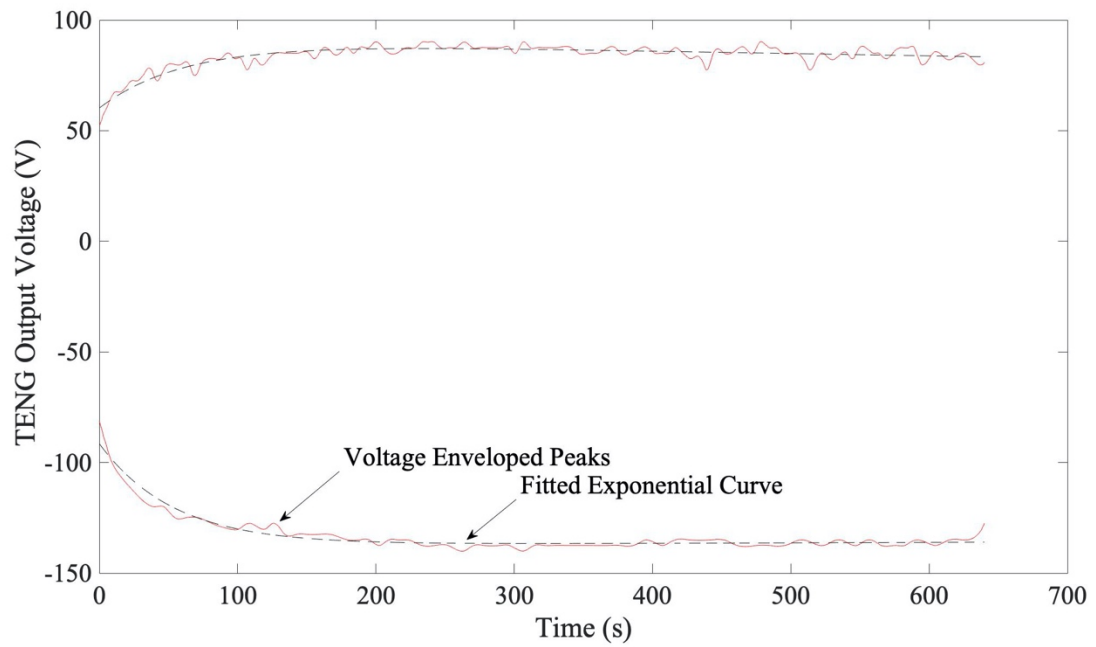


Figure 3.7: An example of TENG voltage output analyzed with positive and negative lines of fit. The solid lines are the positive and negative enveloped voltage peaks. The dashed lines are the line of fits of the positive and negative enveloped peaks.

CHAPTER FOUR
RESULTS AND DISCUSSION

Steady State Charge Comparison

Relative Humidity

The triboelectric energy generator's (TENG's) steady state voltage was compared across the indicated relative humidity range (15%RH -85%RH). The RMS of the TENG voltage output at each relative humidity condition and their averages with error bars, indicating one standard deviation, are plotted in Fig. 4.1.

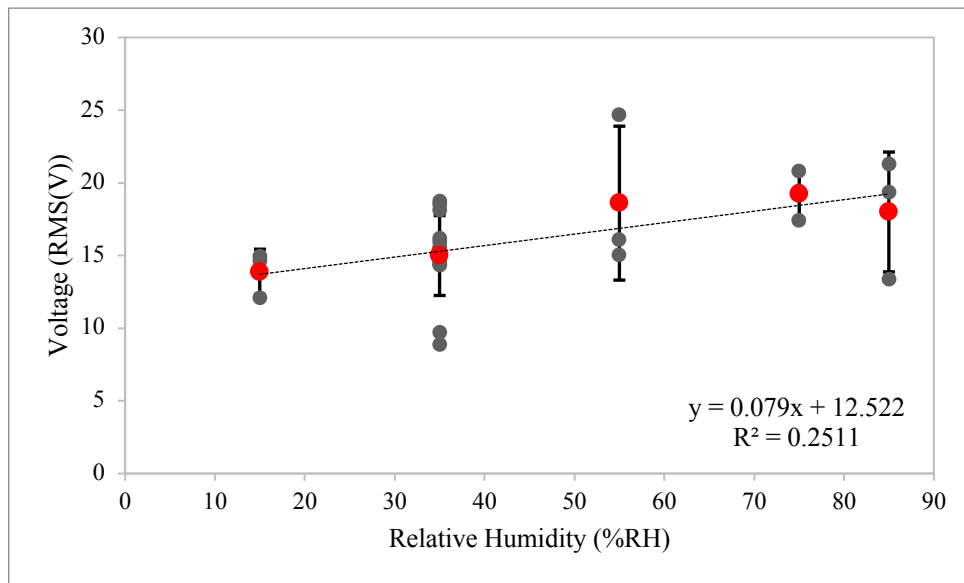


Figure 4.1: TENG steady state RMS voltage during varying relative humidity. The error bars represent one standard deviation. The gray represents all data points. The red represents the average RMS voltage at each relative humidity.

As seen in Fig. 12, the TENG voltage output varied within each relative humidity tested for all three replication runs performed at 15%RH, 55%RH, 75%RH, and 85%RH and all 15 replicate runs performed at 35%RH. The relative humidity with the least variation between tests was 15%RH with a standard deviation of 1.55 volts or 11.21% of the mean 13.88 volts. The relative humidity with the greatest variation was 55%RH with a standard deviation of 5.30 volts or 28.46% of the mean 18.60 volts. These variations presented a challenge in comparing RMS values between conditions. Despite the lack of statistical variation in the TENG output over the range of humidity levels tested, a least squares fit line ($R^2 = 0.25$), Fig. 4.1, was fit to the data and suggested no correlation between relative humidity and TENG output voltage. The only two relative humidity conditions with statistically voltage outputs were 15% RH and 75% RH. This increase in TENG output voltage, as a function of relative humidity increase, was consistent with two of the four previous studies discussed [10, 14, 15, 16], Fig. 4.2.

Out of the four external relative humidity studies, this study's results were closest to Baytekin's study completed in 2011. Baytekin suggested that low humidity conditions would limit contact electrification which is the basis how of TENGs work [16]. This study supports Baytekin's findings that lower humidity conditions result in the TENG having a lower voltage output. However, Baytekin only tested two relative humidity conditions. Pence et al. also had results similar to this study. Pence et al. tested two materials and showed that 0% RH and 90%RH have higher charges compared to the relative humidity condition tests performed at RH levels between 0%RH and 90%RH. While tested under similar RH conditions, one material, [P]-PhSO₃·H⁺, had a consistent

increase in charge from 20%RH to 90%RH which aligns with this study. The other material Pence et al tested, [P]-PhSO₃⁻Na⁺, resulted in a charge decrease from 20%RH to 40%RH and then a charge increase from 40%RH to 90%RH. The second material's results do not align with this study's findings [15]. The remaining two studies that researched the relative humidity effect on triboelectric generators do not support this research [10, 14]. Nguyen stated that as relative humidity increases from 10%RH to 90%RH, the charge decreases which is the opposite of what this study found [14]. Barry et al. stated as relative humidity increases, charge decreases, similar to Nguyen and opposite of what we found [10]. Overall, the results showed the TENG has a consistent voltage output across all of the relative humidities tested. TENGs are a viable power solution throughout the range of relative humidities encountered in the distribution environment without the need for moisture control materials such as vapor barriers and desiccants.








Relative Humidity	Result	Study
	 Charge	(Nguyen, 2013)
	 Charge then  Charge	(Pence, 1993)
	 Charge	(Baytekin 2011)
	 Charge	(Barry, 2016)
	 Steady Charge	(Fisher, 2020)

Figure 4.2: Overview of the studies looking at relative humidity effect on triboelectric energy generators.

Temperature

The triboelectric energy generator's (TENG's) steady state voltage was compared across the indicated temperature range (10°C-30°C). The RMS of the TENG voltage output at each temperature condition and their averages with error bars indicating one standard deviation are plotted in Fig. 4.3.

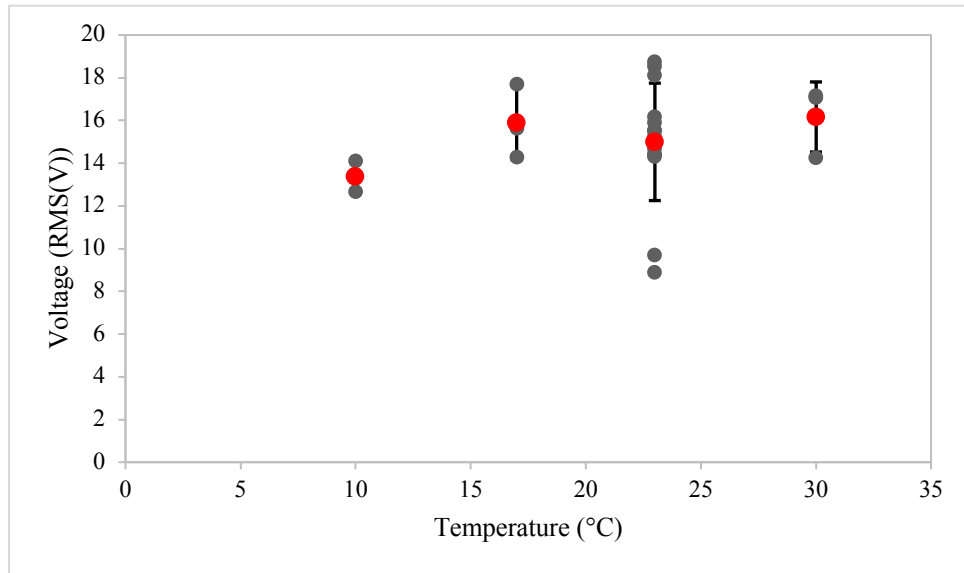


Figure 4.3: TENG steady state RMS voltage during varying temperature. The error bars represent one standard deviation. The gray represents all data points. The red represents the average RMS voltage at each temperature.

As seen in Fig. 4.3, temperature condition tests had large variations within all three repetitions at 10°C, 17°C, and 30°C and all 15 repetitions at 23°C. The TENG output voltage varied the least at 10°C with a standard deviation of 0.73 volts which was 5.47% of the mean 13.36 volts. The TENG output voltage varied the most at 23°C with a standard deviation of 2.75 volts which was 18.33% of the mean 15.00 volts. These data indicated that TENG voltage output did not change as temperatures varied within the packaging distribution environment. There was no statistical difference with the TENG output when considering the mean of the RMS voltages at each temperature. Unlike with the varied relative humidity testing, there was not a discrete trend in the TENG output

over the temperature range tested. Overall, these results support that TENG voltage output was not affected in the temperature range 10°C – 30°C.

These results closely mirror Lu et al.’s results from 2017. Lu et al. also did not see a large variation of TENG voltage output within the packaging distribution temperature range that was tested. The data collected in the 10°C and 17°C range showed slight variation between Lu et al.’s and this study. Lu et al. showed that temperatures lower than ~20°C have a slightly higher voltage output than temperatures in the packaging distribution range, which is opposite of this data set [17]. Xu et al.’s study on temperature and TENG output performance was drastically outside of the packaging distribution temperature range and therefore not comparable [18]. An overview of these studies is shown in Fig. 4.4.





Temperature	Result	Study
 Temperature	 Charge then overall steady	(Lu, 2017)
	 Charge (extremely high temperatures)	(Xu, 2018)
	 Steady Charge	(Fisher, 2020)

Figure 4.4: Overview of the studies looking at temperature effect on triboelectric energy generator output performance.

Transient Charge Comparison

The triboelectric energy generator (TENG) charge build up was compared across the relative humidity range (15%RH -85%RH) and temperature range (10°C-30°C). A

two-term exponential curve, Eq. (3.1), was fit to each of the positive and negative peak envelopes for the first 10.66 minutes. All of the relative humidity conditions' lines of fit and temperature conditions' lines of fit were plotted in Fig. 4.5 and 4.6 respectively. The rate of charge build up was greatest in the first 100 seconds of the all tests across all conditions.

In the positive peak curves of the relative humidity tests, all 15%RH curves were within the bottom half of the data set and all 75%RH and 85%RH curves were within the top half of the data set, Fig. 4.5. The highest (most positive) relative humidity positive peak curve was 35%RH, and the lowest curve was 85%RH.

The negative (bottom) relative humidity tests resulted in the 75%RH and 85%RH data making up the bottom (most negative) six curves, Fig. 4.5. The remaining data within the relative humidity negative peak curves had no correlation. The least negative curve was 85%RH, while the most negative curve was 15%RH. The positive and negative peak curves align with the trend seen in the steady state comparison. The trend shows that the higher relative humidities visually have larger voltages; however statistically there is no difference in voltage output between relative humidity conditions.

In the temperature positive peak graph, Fig. 4.6, all of the 30°C tests made up three out of top five highest curves with the remaining temperature data in no pattern. The highest curve was 23°C, while the lowest positive curve was 23°C.

The negative temperature peak data resulted in the 30°C tests being included in three out of the four lowest (most negative) curves. In the negative temperature peak curves, the lowest curve was 23°C while the highest (least negative) curve was 23°C.

The positive and negative peak curves of various temperatures align with the trends seen in the steady state comparison. The trends show that the higher temperatures visually and statistically have no voltage differences between temperature conditions.

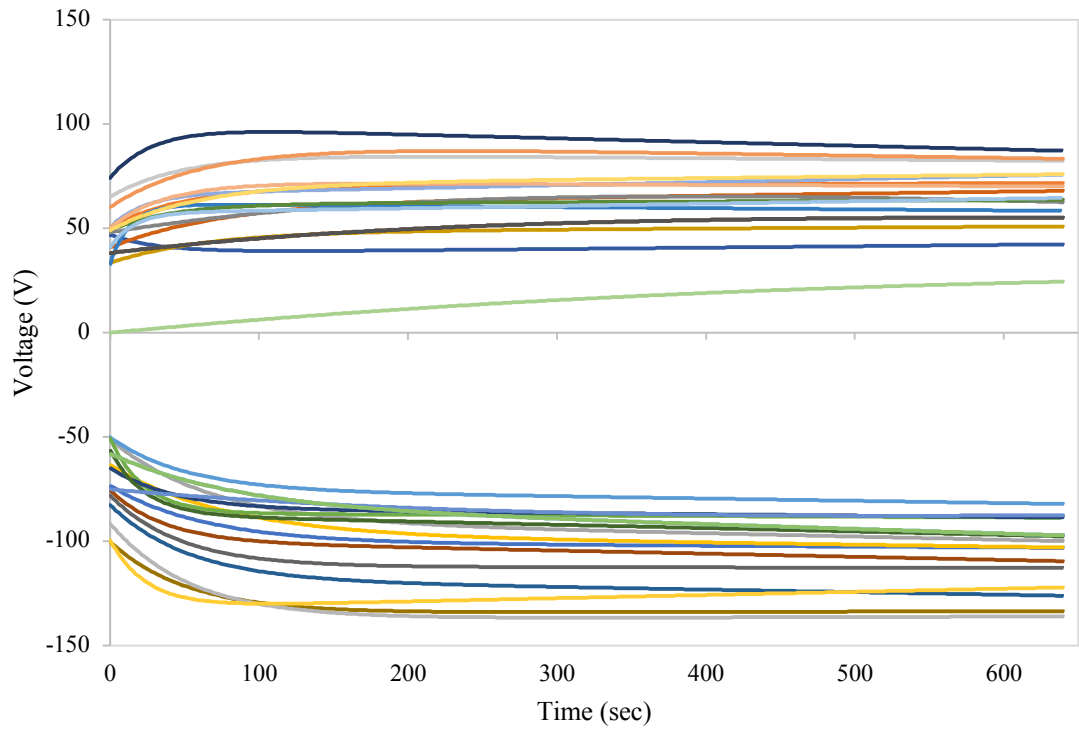


Figure 4.5: Relative humidity condition lines of best fit charge build up.

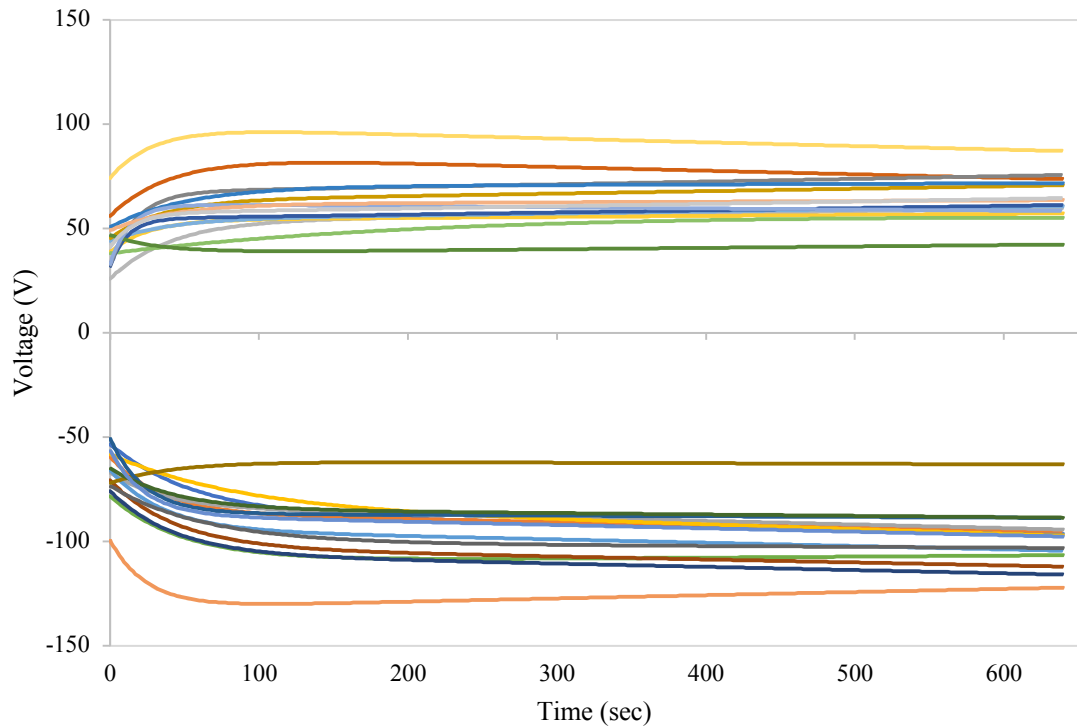


Figure 4.6: Temperature condition lines of best fit charge build up.

The four coefficients from each line of best fit equation were compared using a MANOVA test. The MANOVA test was performed on each of the following data sets: positive relative humidity conditions' coefficients, negative relative humidity conditions' coefficients, positive temperature conditions' lines of fit, and negative temperature conditions' lines of fit. Each test generated a p-value that was analyzed to determine if there was a statistically significant change in the coefficients of the two-term exponential curves fit to the peak envelopes. The MANOVA tests are presented in Table 4.1.

Table 4.1: The MANOVA test results.

MANOVA Test	p-value
Positive Relative Humidity Curves	0.46
Negative Relative Humidity Curves	0.17
Positive Temperature Curves	0.35
Negative Temperature Curves	0.14

Since the p-values are all above 0.05, it was concluded that charge build up performance for this TENG cannot be shown to be dependent upon humidity or temperature. An alpha (α) of 0.05 was used to analyze the MANOVA tests and represents a confidence level of 95%. The confidence level indicated the percentage of all the samples expected to be in the true population parameter [25]. The closest p-values to the alpha (α) of 0.05 were the negative voltages of both the relative humidity and the temperature tests. The positive voltage peaks of the relative humidity and temperature tests had the highest p-values. This study was one of the first studies to compare TENG charge build up over time. Previous published research stated TENG charge build up was a few hundred cycles long before reaching stabilization [7].

Most of the previous research compared TENG voltage output of different relative humidity and temperature conditions using single numerical values, making it difficult to compare these results to past works [10, 14, 15, 16, 17]. Only one study, by Xu et al. in 2018, looked at charge over time; however, this study looked at charge over time at extremely high temperatures. Xu et al.'s temperature conditions are not within

the packaging distribution range, and therefore not comparable [18]. Overall, this study determined that there is not a change in charge build up when comparing lines of best fit across relative humidity conditions or temperature conditions; however the charge build up before equilibrium was longer than previous works suggested [7, 14, 24, 26].

Previous researchers [14, 24, 26] had accepted that TENGs reach equilibrium after a “few hundred” cycles, just as Saurenbach suggested, with no further research completed [7]. This TENG experienced a double impact with an input of 5 Hz during testing and thus took around 30 seconds to reach 300 cycles of impacts. As seen in Figures 10 and 11, at around 30 seconds, the steepest part of the charge build up curve has passed for most of the tests. The voltage was still increasing throughout the remainder of the first recording, 10.66 minutes. This data showed no charge equilibrium within the first 10.66 minutes of testing, approximately 6400 cycles of impacts, which is more than the few hundred cycles suggested by Saurenbach [7]. This findings implied that charge build up time extends past the original estimate of a few hundred cycles.

CHAPTER FIVE

CONCLUSION

The trend in increase in data collection and the need for more sensors in place to power the data collection drives the research in triboelectric energy generators (TENGs) [1]. When using TENGs for sensor power in the packaging distribution environment, there are environmental conditions experienced by packaged products that should be considered for optimum TENG output. There are two main environmental conditions that are considered in this paper: relative humidity and temperature. Relative humidity ranges in a packaging distribution environment typically vary from 15%RH – 85%RH, with some data pointing slightly outside of this range [11, 12, 13]. Temperature ranges in a packaging distribution environment typically vary from -29°C to 60°C with some temperatures slightly outside this range [11, 12]. This study tested a TENG using a custom-built environmental chamber mounted on an electrodynamic shaker for a sinusoidal input. The goal of this study was to determine the effect of relative humidity and temperature on the charge accumulation and steady state performance of a triboelectric energy generator.

A steady state, root mean square (RMS) voltage comparison was performed to explore the TENG voltage output at relative humidity and temperature range seen within a packaging distribution environment. As humidity increased from 15%RH to 85%RH, overall, the TENG RMS voltage remained consistent and did not have a correlation between relative humidity and RMS voltage. However, visually, there was a slight increase in voltage output with increasing temperature. As temperatures increased from

10°C to 30°C, the TENG average voltage output remained consistent. In other words, within the packaging distribution environment, this work suggests that TENG performance is consistent over a wide range of relative humidity and temperature. These results show that TENGs can be used to power devices in a packaging distribution environment. When using a TENG throughout the distribution environment, there is no need to shield or control relative humidity or temperature through the use of barrier films or desiccants.

A charge build up comparison that explored the TENG voltage output over the first 10.66 minutes of each test run, at varying relative humidities and temperatures, within the packaging distribution environment was performed. The positive and negative voltage peaks were analyzed and ultimately a two-term exponential curve was fit to the positive and negative charge build envelope. The four coefficients for each two-term exponential curve were compared using a multivariate analysis of variance (MANOVA) test. Upon comparison of these lines of fit, charge build up did not change based on relative humidity or temperature. While analyzing the charge build up, the results showed charge equilibrium might not happen within a few hundred cycles as one previous study predicted and other studies have accepted as a basis for work. This study found in the first 10.66 minutes, approximately 6400 cycle impacts, the charge was still slightly increasing for most tests.

This research compared steady voltage output with varying relative humidities over the same temperature, 35°C, and steady voltage output with varying temperatures over the same relative humidity, 35%RH with a vertical contact and separation TENG.

Further research could be done with varying relative humidities and temperatures over different consistent relative humidities and temperatures. With these additional data points, a 3D plot comparing varying relative humidities with varying temperatures. In addition to more temperatures and relative humidities, more work could be done investigating other modes of TENGs for a packaging application. Different modes of TENGs have different advantages and thus could be used in different ways than vertical-contact and separation mode.

In summary, relative humidity and temperature ranges within the packaging distribution environment do not affect the steady state TENG voltage output and charge build up. This study shows a TENG can be depended on for voltage generation across a wide range of environmental conditions.

APPENDICES

Appendix A

Triboelectric Energy Generator Setup

The triboelectric energy generator (TENG) used in this study was created by the Advanced Dynamics and Mechanics (ADAMS) lab at Purdue University and seen in Fig. A-1. The generator was 3D printed on an Ultimaker S5 desktop 3D printer out of polylactic acid (PLA). The TENG was custom made to attach to the electrodynamic (ED) shaker's expander head and when assembled, had overall dimensions of 97.5 x 150 x 300 mm as indicated in Fig. A-1. The PLA TENG generator had five holes in the base to allow for screws to hold the generator securely in place throughout testing. On the back region of the TENG, there was a 300 mm linear guide rail mounted with screws. This guiderail allowed the top moving platen of the TENG to experience minimal friction. The weight of the assembled generator with no additional top platen mass was 393 g. The top moving platen had a 200 g mass mounted to the center. In order to measure the movement of the top platen, a piezoelectric accelerometer (PCB, Depew, NY) was mounted directly beside the 200 g mass using super glue. The excitation input for the assembled generator with the 200 g mass was 1.4 +/- 0.05g at 5 Hz to maximize contact, separation and voltage output of the TENG. The platen materials (Copper, Nylon 6,6, and PTFE (Teflon)) selection was discussed above in the thesis body. The platen materials were attached to each platen using 3M spray adhesive. The 3M spray adhesive was used as an adhesive strong enough to ensure materials remained attached throughout the whole test.

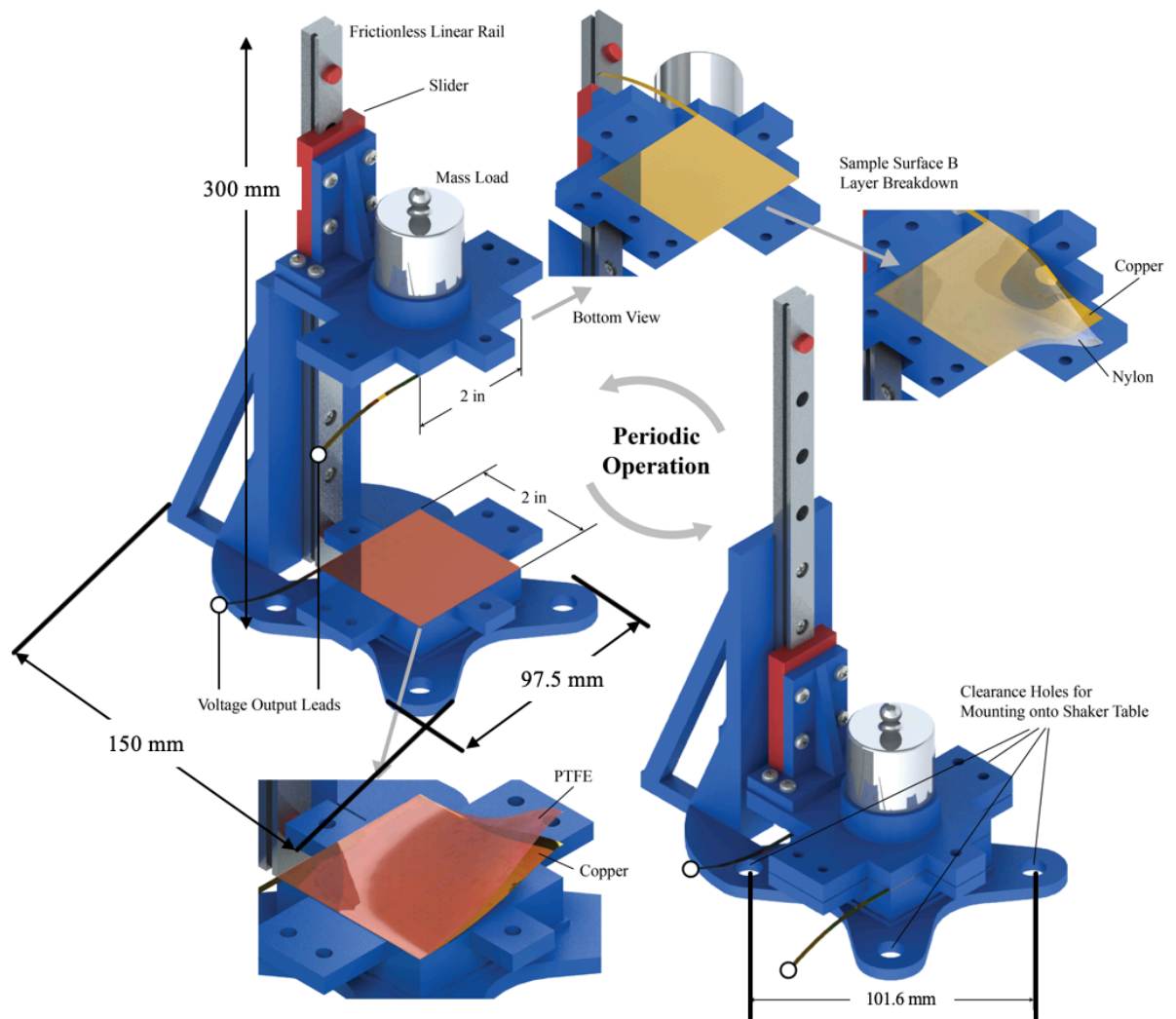


Figure A-1: A detailed diagram of the triboelectric energy generator created at Purdue University.

Appendix B

The Hysteresis Effect in Triboelectric Energy Generators

While material selection was important for the contact surfaces, the material of the generator's moving platens was also crucial. The original set up of the generator included platens made of 9mm thick thermoplastic polyurethane (TPU) attached to the upper and lower polylactic acid (PLA) platens. TPU was used for mounting the contact materials, Nylon 6,6, Teflon, and Copper, as seen in Figure A-2.1. The initial reasoning behind TPU was utilizing a softer material to ensure complete contact with the top and bottom platens; however, after initial testing, TPU was found to further complicate the triboelectric energy generator (TENG) dynamics. The viscoelastic material exhibited a hysteresis effect.

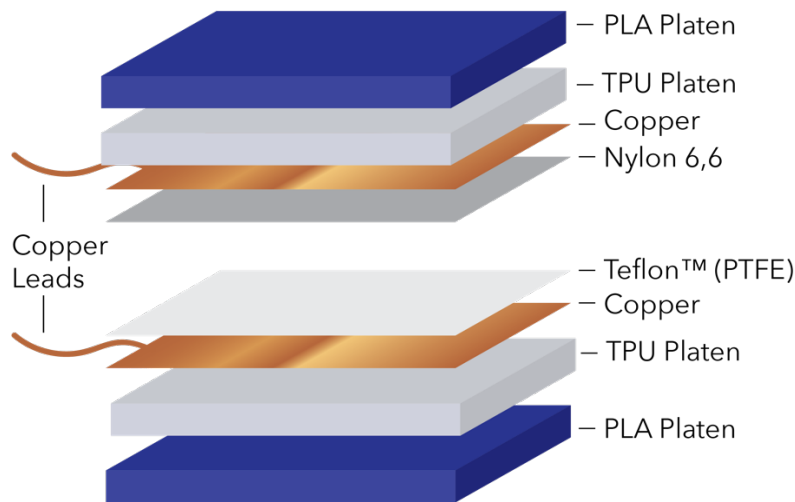


Figure A-2.1: Initial set up of the two triboelectric generator platens that experienced hysteresis effect.

The hysteresis effect is defined as “the phenomenon in which the value of a physical property lags behind changes in the effect causing it” [27]. The hysteresis effect

was seen in the accelerations of the top moving TPU platen. The acceleration, especially the positive accelerations, of the moving platen increased over the first 250 seconds, when given a consistent input from the electrodynamic (ED) shaker as seen in Figure A-2.2. The increase in acceleration of the top moving platen over time made it difficult to compare charge build up over time because the accelerations were not consistent during a time period. In order to eliminate the hysteresis effect and ensure consistent acceleration over time, TPU was removed from the PLA platens and the contact materials, Nylon 6,6, Teflon, and Copper, were mounted directly to PLA platens instead. Since PLA was a harder material compared to TPU, PLA was utilized to eliminate the hysteresis phenomenon and supported consistent accelerations over time as seen in Figure A-2.3. The PLA change from positive to negative accelerations were greater than the TPU accelerations, which was expected because PLA is stiffer than TPU. The final platens set up had no TPU and was entirely made of PLA, Nylon 6-6, Teflon, and Copper as seen in Figure A-2.4.

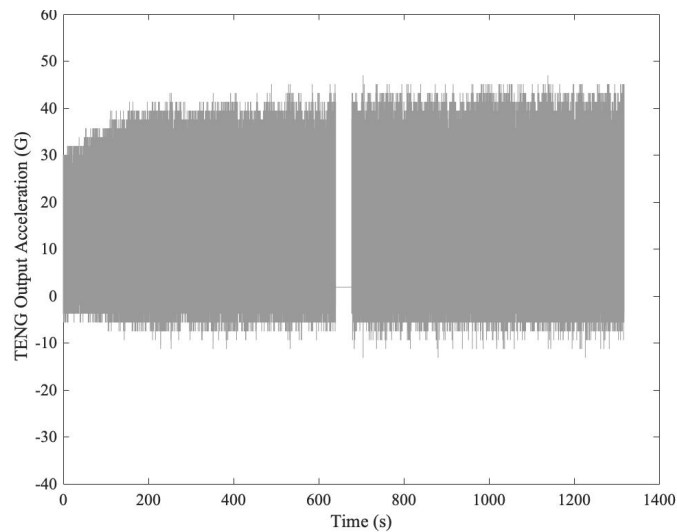


Figure A-2.2: Example of hysteresis effect of the platens made with TPU.

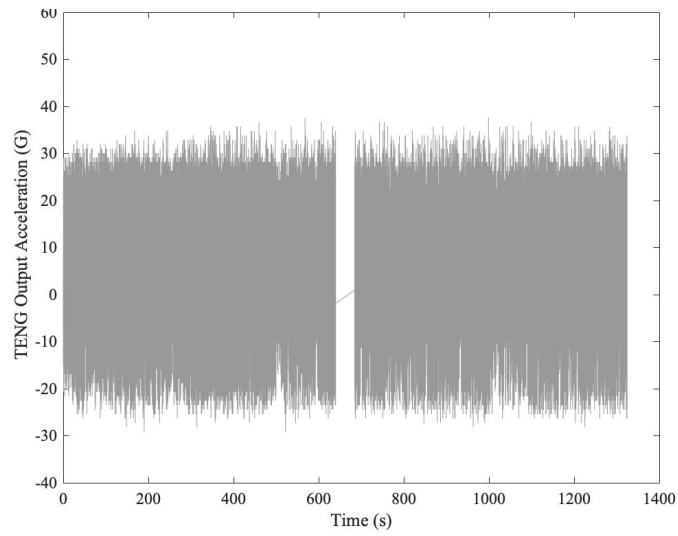


Figure A-2.3: Example of no hysteresis effect of the platens made with PLA.

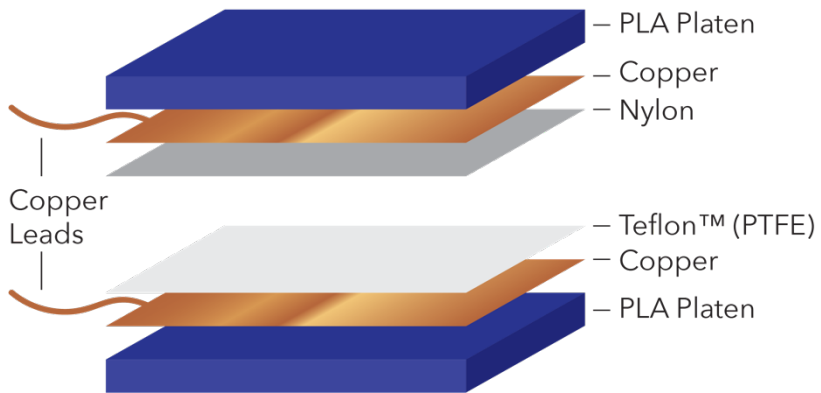


Figure A-2.4: Final set up of the two triboelectric generator platens that does not experience hysteresis effect.

REFERENCES

- [1] J. Paulsen, "Enormous Growth in Data is Coming - How to Prepare for It, and Prosper From It," 2019. [Online]. Available: <https://blog.seagate.com/business/enormous-growth-in-data-is-coming-how-to-prepare-for-it-and-prosper-from-it/>. [Accessed 9 November 2019].
- [2] S. Boiseau, B. Despesse and B. Ahmed Seddik, "Electrostatic Conversion for Vibration Energy Harvesting," *Small-Scale Energy Harvesting*, 2012.
- [3] Z. L. Wang and J. H. Song, "Nanogenerators Based on Zinc Oxide Nanowire Arrays," *Science*, April 2006.
- [4] Z. Wang, "Triboelectric Nanogenerators as New Energy Technology for Self-Powered Systems and as Active Mechanical and Chemical Sensors," *ACS Nano*, vol. 7, no. 11, pp. 9533-9557, 2013.
- [5] A. Diaz and R. Felix-Navarro, "A semi-quantitative triboelectric series for polymeric materials: The influence of chemical structure and properties.," vol. 62, no. 4, pp. 277-290, 2004.
- [6] Z. Wang, J. Chen and L. Lin, "Progress in triboelectric nanogenerators as a new energy technology and self-powered sensors," *Energy & Environmental Science*, no. 8, pp. 2250-2282, 2015.
- [7] F. Saurenach, D. Wollmann, B. Terris and A. Diaz, "Force Microscopy of Ion-Containing Polymer Surfaces: Morphology and Charge Structure," *Langmuir*, vol. 8, pp. 1199-1203, 1992.
- [8] G. Zhu, B. Peng, J. Chen, Q. Jing and Z. Wang, "Triboelectric Nanogenerators as a New Energy Technology: From fundamentals, devices, to applications," *Nano Energy*, vol. 14, pp. 126-138, 2015.
- [9] C. Wu, A. Wang, W. Ding, H. Guo and Z. Wang, "Triboelectric Nanogenerator: A Foundation of the Energy for the New Era," *Advanced Energy Materials*, vol. 9, no. 1, 2018.
- [10] A. Barry, G. Batt, D. Darby and J. Gibert, *The Application of a Triboelectric Energy Harvester in the Packaged Product Vibration Environment*, Clemson: Clemson University, 2016.

- [11] International Safe Transit Association, "ISTA 3B 2013," in *ISTA 2018 Resource Book*, 2018.
- [12] D. Leinberger, "Temperature & Humidity in Ocean Containers," Xerox Corporation, Wilsonville, 2006.
- [13] NOAA Weather Station Raw Data, "Greenville-Spartanburg International Airport, SC US (WBAN: 03870)," October 2018. [Online]. [Accessed 1 April 2019].
- [14] V. Nguyen and R. Yang, "Effect of humidity and pressure on the triboelectric nanogenerator," *Nano Energy*, vol. 2, no. 5, pp. 604-608, 2013.
- [15] S. Pence, V. Novotny and A. Diaz, "Effect of Surface Moisture on Contact Charge of Polymers Containing Ions," *Langmuir*, vol. 10, pp. 592-596, 1994.
- [16] H. Baytekin, B. Baytekin, S. Soh and B. Grysowski, "Is water necessary for contact electrification?," *Angewandte Chemie*, vol. 50, pp. 6766-6770, 2011.
- [17] C. Lu, C. Han, G. Gu, J. Chen, Z. Yang, T. Jiang, C. He and Z. Wang, "Temperature Effect of Performance of Triboelectric Nanogenerator," *Advanced Engineering Materials*, vol. 19, no. 12, 2017.
- [18] C. Xu, Y. Zi, A. Wang, H. Zou, Y. Dai, X. He, P. Wang, Y. Wang, P. Feng, D. Li and Z. Wang, "On the Electron-Transfer Mechanism in the Contact-Electrification Effect," *Advanced Materials*, vol. 30, no. 15, 2018.
- [19] F. Galembak, T. Burgo, L. Balestrin and R. Gouvia, "Friction, Tribochemistry, and Triboelectricity: Recent Progress and Perspectives," *RSC Adv.*, pp. 64280-64298, 2014.
- [20] International Safe Transit Association, "ISTA History and Mission," [Online]. Available: https://ista.org/history_mission.php. [Accessed August 2019].
- [21] D. Goodwin and D. Young, *Protective Packaging for Distribution: Design and Development*, DEStech Publications, Inc, 2010.
- [22] Y. Su, J. Chen, Z. Wu and Y. Jiang, "Low temperature dependence of triboelectric effect for energy harvesting and self-powered active sensing," *Appl. Phys. Lett.*, vol. 106, 2015.
- [23] H. Zou, Y. Zhang, L. Guo, P. Wang, X. He, G. Dai, H. Zheng, C. Chen, A. Wang, C. Xu and Z. Wang, "Quantifying the triboelectric series," *Nature Communications*, 2019.

- [24] M. Seol, J. Woo, D. Lee, H. Im, J. Hur and Y. Choi, "Nature-Replicated Nano-in-Micro Structures for Triboelectric Energy Harvesting," *Small*, vol. 10, no. 19, pp. 3887-3894, 2014.
- [25] Stat Trek, "Statistics Dictionary - Confidence Level," Stat Trek, [Online]. Available:
https://stattrek.com/statistics/dictionary.aspx?definition=confidence_level.
[Accessed May 2020].
- [26] S. Wang, L. Lin and Z. Wang, "Nanoscale Triboelectric-Effect-Enabled Energy Conversion for Sustainably Powering Portable Electronics," *Nano Letters*, vol. 12, no. 12, pp. 6339-6346, 2012.
- [27] "Hysteresis," Lexico Powered by Oxford, [Online]. Available:
<https://www.lexico.com/en/definition/hysteresis>. [Accessed 8 May 2020].